J. Condensed Matter Nucl. Sci. 5 (2011) 116–139

Research Article

Coherent Energy Exchange in the Strong Coupling Limit of the Lossy Spin-Boson Model

Peter L. Hagelstein *

Research Laboratory of Electronics, Massachusetts Institute of Technology, Cambridge, MA 02139, USA

Irfan U. Chaudhary

Department of Computer Science and Engineering, University of Engineering and Technology. Lahore, Pakistan

Abstract

We focus on the lossy spin-boson model since it is capable of efficient energy exchange between two-level systems and an oscillator under conditions where the characteristic energy of the oscillator is small compared to the transition energy of the two-level systems. We are considering this model as the essential component for a theoretical understanding of the excess heat effect in the Fleischmann–Pons experiment. We introduce an iterative algorithm that allows the numerical calculation of eigenfunctions and eigenvalues of the coefficient eigenvalue equation that arises in the local approximation. From systematic calculations in the strong coupling limit we establish scaling laws for the self-energy and for the indirect coupling matrix element in the local approximation. These results are used to study the system dynamics for simple strong coupling models.

Keywords: Coherent energy exchange, Excess heat, Fleischmann–Pons experiment, Lossy spin-boson model, Theory

1. Introduction

In this work we continue our studies of coherent energy exchange between a set of two-level systems and an oscillator, under conditions where the transition energy of the two-level systems is much greater than the characteristic energy of the oscillator. Our interest in this problem is motivated by a great many experiments in which positive results have been reported on measurements of excess heat in the Fleischmann–Pons effect [1,2]. In these experiments a very large amount of energy is sometimes produced, with no sign of chemical or material changes commensurate with the energy produced. Fleischmann and Pons conjectured that the origin of the energy was nuclear; however, known exothermic nuclear reactions that produce energy do so through energetic particles, and there are no commensurate energetic

*E-mail: plh@mit.edu

particles in the Fleischmann–Pons experiment. Helium has been observed correlated with the energy [3–5], and the ratio of energy produced to helium observed is near 24 MeV [6]. This is significant since it is consistent with the mass difference between two deuterons and a ^{4}He nucleus.

Hence, experiment suggests that the energy is probably nuclear in origin, and that perhaps deuterons are somehow reacting to make ^{4}He. The big problem with such a statement is that there are no previous examples in nuclear physics of nuclear reactions making energy without commensurate energetic particles [7]. So, whatever process that is responsible for the effect is one that hasn't been seen before. There are no previous relevant models in the nuclear physics or condensed matter physics literature, and most scientists believe the literature that does exist rules out any possibility of such an effect.

This situation would change radically if there were a known mechanism which could take a large nuclear scale MeV quantum and convert it efficiently into a large number of optical phonons. Such a scenario would be consistent with recent two-laser experiments [8,9], where two weak lasers incident on the cathode surface initiate an excess heat event when the beat frequency is matched to zero-group velocity point of the optical phonons, and the excess heat persists after the lasers are turned off. The excess heat effect initiated with a single laser does not persist. The picture which has been proposed to account for this is one in which the two lasers provide an initial excitation of the optical phonon modes which the new process requires; then, when the lasers are turned off, the new process channels energy into the same modes which sustains the effect.

To make progress given such a picture, we need to understand the conditions under which a large nuclear energy quantum can be converted into a large number of optical phonons. Once again, there is no precedent for this; however, it does seem to be what is going on in these experiments, and this motivates us to explore theoretical models which exhibit such an effect. Coherent energy exchange as a physical effect under conditions where are large quantum is divided into many smaller quantum is known in NMR and in atomic physics; it is predicted in the spin-boson model. However, the effect in the spin-boson model is weak, and we need a much stronger version of it to make progress with the excess heat effect in the Fleischmann–Pons effect.

When we augment the spin-boson model with loss, we see that the coherent energy exchange process improves dramatically [10]. In perturbation theory we see that this comes about through the removal of destructive interference, which drastically hinders the effect in the basic spin-boson model. In a set of recent papers [10–13], we have been discussing the model, and building up tools and results to try to understand coherent energy exchange when the coupling is stronger and when more quanta are exchanged. In the preceding paper [13], we introduced the local approximation for the lossy spin-boson model, which provides us with a powerful tool with which to address the strong coupling regime.

In this work, we continue the analysis by first introducing a numerical algorithm which allows us to obtain eigenfunctions, self-energies, and indirect coupling matrix elements in the strong coupling regime. As will be discussed, once we began assembling the results from systematic calculations we noticed that the system appeared to obey scaling laws in the strong coupling regime. This is interesting because after establishing the scaling laws, we can use them to predict the dynamics of the model under conditions of extremely strong coupling, which is where we need to go in order to convert a nuclear-scale quantum into a very large number of atomic scale quanta. Our primary goal then in what follows in this paper is to discuss the scaling laws for self-energy and for the indirect coupling matrix element in the strong coupling regime.

2. Eigenvalue Equation for the Coefficients

We are interested in coherent energy exchange in the lossy spin-boson model under conditions where the coupling is strong, and where a great many oscillator quanta are exchanged for each two-level system transition. In our earlier discussions of the problem, we have introduced a number of models and approximations which allow us to make

progress on what would otherwise be a difficult theoretical problem. For example, if we assume that the loss is infinite for states below a certain energy and adopt a restricted basis approximation, then we obtain a reduced version of the problem that has fewer states and leads to a real Hamiltonian and real solutions. In the local approximation, we assume that the matrix elements change little when the number of excited two-level systems is increased or decreased. When the resonance conditions is met, then the Hamiltonian becomes invariant under translation, and by Bloch's theorem the solutions are periodic in one dimension. This further simplifies things, and allows us here to analyze the system in regimes closer to those of interest for understanding excess heat in the Fleischmann–Pons effect.

2.1. Local approximation eigenvalue equation

We begin with the eigenvalue equation for the expansion coefficients that was developed previously [13] for the local approximation

$$E(\phi)v_n = \left[n\hbar\omega_0 - i\frac{\hbar}{2}\hat{\Gamma}(E)\right]v_n + g\Delta E\left[e^{i\phi}(v_{n+\Delta n+1} + v_{n+\Delta n-1}) + e^{-i\phi}(v_{n-\Delta n+1} + v_{n-\Delta n-1})\right]. \quad (1)$$

In this equation, ΔE is the transition energy of the two-level systems, $\hbar\omega_0$ is the characteristic oscillator energy, g is the dimensionless coupling constant, and ϕ is the phase associated with the Bloch solutions of the periodic problem that results when the resonance condition

$$\frac{\Delta E}{\hbar\omega_0} = \Delta n \quad (2)$$

is satisfied for odd integer Δn. Loss is included in general in this model through the second-order loss operator $i\hbar\hat{\Gamma}(E)/2$. In this paper our focus will be on the infinite loss model (in a restricted basis approximation), so that we will take v_0 to be to lowest expansion coefficient that is finite. As in our previous work, we assume that the oscillator is very highly excited, so that the oscillator index n is incremental. The number of oscillator quanta to be associated with v_0 is n_0, which we assume is very large; the total number of oscillator quanta in general associated with v_n is then $n_0 + n$.

2.2. Focus on the $\phi = 0$ and $\phi = \pi$ problems

We are interested in the self-energy and in the indirect coupling matrix element. As discussed in [13] it is easier to compute the level splitting, from which we can estimate the nearest neighbor indirect coupling matrix element. For this, we need two eigenvalues $E(0)$ and $E(\pi)$. The corresponding eigenvalue equations can be written as

$$\epsilon_0 v_n = \frac{n}{\Delta n}v_n + g\left[(v_{n+\Delta n+1} + v_{n+\Delta n-1}) + (v_{n-\Delta n+1} + v_{n-\Delta n-1})\right], \quad (3)$$

$$\epsilon_\pi v_n = \frac{n}{\Delta n}v_n - g\left[(v_{n+\Delta n+1} + v_{n+\Delta n-1}) + (v_{n-\Delta n+1} + v_{n-\Delta n-1})\right], \quad (4)$$

where

$$\epsilon_0 \;=\; \frac{E(0)}{\Delta E}, \qquad \epsilon_\pi \;=\; \frac{E(\pi)}{\Delta E}. \tag{5}$$

3. Solutions for Moderately Large Δn

To extend our results significantly beyond what was done in our earlier papers we require new numerical and analytical tools. In this section we present an iterative numerical approach which allows us to develop solutions to the eigenvalue equations under conditions where a direct solution is impractical. This allows us study coherent energy exchange when a two-level system quantum is split into a moderately large number of oscillator quanta. The results of such calculations are interesting since we find that the indirect coupling matrix element appears to obey a useful scaling law.

3.1. Matrix eigenvalue problem

When the resonance condition is satisfied in the local approximation, we obtain an eigenvalue equation for the expansion coefficients of the form

$$\epsilon_0 v_n \;=\; \frac{n}{\Delta n} v_n + g\Big[(v_{n+\Delta n+1} + v_{n+\Delta n-1}) + (v_{n-\Delta n+1} + v_{n-\Delta n-1}) \Big]. \tag{6}$$

In the restricted basis approximation of the lossy spin-boson model with infinite loss, we assume that the expansion coefficients with n negative are zero due to loss effects. Here Δn is an odd integer, which is the number of quanta exchanged on resonance, and g is the dimensionless coupling constant.

This eigenvalue equation for the expansion coefficients can be thought of as a matrix eigenvalue equation of the form

$$\epsilon \mathbf{v} \;=\; \mathbf{H} \cdot \mathbf{v}. \tag{7}$$

3.2. Iterative numerical scheme

When the vector $\mathbf{v}$ has more than 1000 elements, the matrix eigenvalue problem that results becomes computationally expensive for a direct calculation. As a result, we seek an iterative numerical scheme that is faster, which will allow us to extend our computations to examples with larger Δn and strong coupling.

We have found that the computations can be improved considerable with the use of Newton's method with an inequivalent Jacobian. Although the method in general was developed to handle nonlinear problems, it is possible to use it on a linear problem. We begin by assuming that the exact solution can be obtained by adding a small correction to a current guess, such that

$$\mathbf{v}_{\text{exact}} \;=\; \mathbf{v} + \delta\mathbf{v}. \tag{8}$$

If so, then we can develop an exact equation for the correction $\delta\mathbf{v}$ of the form

$$(\mathbf{H} - \epsilon) \cdot \delta\mathbf{v} \;=\; -(\mathbf{H} - \epsilon) \cdot \mathbf{v}. \tag{9}$$

The term on the RHS we recognize as a residual for this problem, which we define as

$$\mathbf{r} \;=\; (\epsilon - \mathbf{H}) \cdot \mathbf{v}. \tag{10}$$

This vector keeps track of how far away from the exact solution the current guess is. We see that the residual goes to zero when we have an exact solution for ϵ and $\mathbf{v}$. The correction $\delta\mathbf{v}$ then satisfies

$$(\mathbf{H} - \epsilon) \cdot \delta\mathbf{v} \;=\; \mathbf{r}. \tag{11}$$

Unfortunately, the amount of work required to evaluate the correction $\delta\mathbf{v}$ is considerable as written. However, we can gain an advantage if we can find an approximate version of $\mathbf{H}$ that we can solve more efficiently. Suppose that this approximate matrix is defined to be $\mathbf{A}$, and that

$$\mathbf{A} \;\approx\; \mathbf{H} \tag{12}$$

in some computationally useful sense. Then the correction $\delta\mathbf{v}$ will no longer be exact, but it may still improve $\mathbf{v}$ anyway. This leads to the following iterative scheme

$$[\mathbf{A} - \epsilon^{(m)}] \cdot \delta\mathbf{v}^{(m)} \;=\; \mathbf{r}^{(m)}, \tag{13}$$

$$\mathbf{v}^{(m+1)} \;=\; \mathbf{v}^{(m)} + \beta\delta\mathbf{v}^{(m)}, \tag{14}$$

$$\epsilon^{(m+1)} \;=\; \frac{(\mathbf{v} \cdot \mathbf{H} \cdot \mathbf{v})^{(m+1)}}{(\mathbf{v} \cdot \mathbf{v})^{(m+1)}}, \tag{15}$$

where β is an under-relaxation parameter.

We have found that corrections can be made with an approximate Hamiltonian that corresponds to

$$\epsilon\delta v_n \;=\; \frac{n}{\Delta n}\delta v_n - \alpha g(\delta v_{n+2} + \delta v_{n-2}) - r_n. \tag{16}$$

We have used the parameter values

$$\alpha \;=\; 0.5, \quad \beta \;=\; 0.5. \tag{17}$$

3.3. Selected results

We have computed results for two examples with $\Delta n = 91$ and with $\Delta n = 151$. These examples are instructive in that the number of oscillator quanta exchanged now is significantly larger than what we have presented previously, and the results already appear to show the presence of nontrivial scaling laws. We show the self-energy in Fig. 1. The two curves are very close to each other, and are roughly linear in g. For large g the curves approach

$$\frac{E(g)}{\Delta E} \;\rightarrow\; -4g. \tag{18}$$

We recall that when the indirect coupling is weak that the indirect matrix element $V_{\rm eff}$ is related to the level splitting through

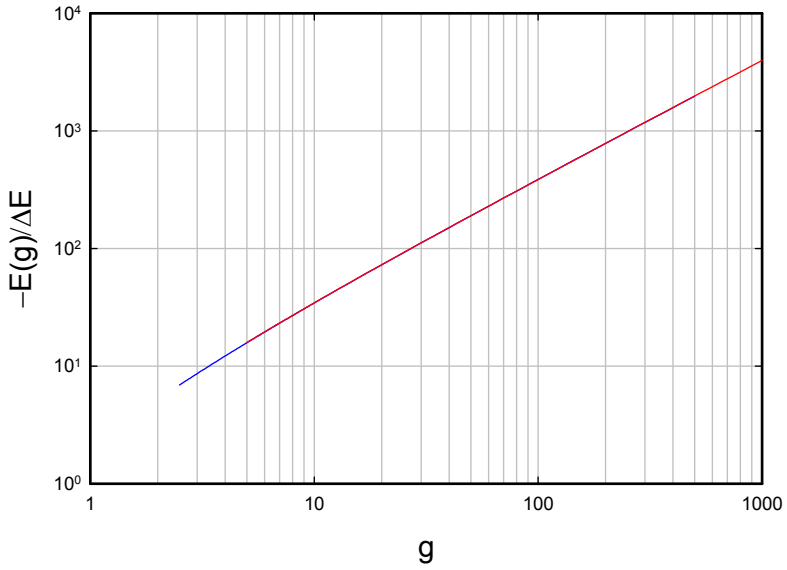

Figure 1. Self-energy as a function of the dimensionless coupling strength g for $\Delta n = 91$ (blue) and $\Delta n = 151$ (red).

$$V_{\rm eff} \;\rightarrow\; \frac{E(0) - E(\pi)}{4}. \tag{19}$$

We have computed the level splitting for the two examples for different values of g, and we have found that the results approximately line up if we plot $\Delta n^2 V_{\rm eff}/4g\Delta E$ (which is a scaled version of $V_{\rm eff}$) as a function of $g/\Delta n^2$ (which is a scaled version of g). The results are shown in Fig 2. This is our first indication so far that the solutions obey an important scaling law in this regime.

The expansion coefficients v_n are shown in Fig. 3 for models with different values of g, for the case where $\phi = 0$. We see peaks with an alternating sign that appear every $\Delta n = 91$ in n, with amplitudes that decrease at large n. The coupling present in the Hamiltonian results in phase coherence that extends over a large range of n. When the coupling is stronger we see that more expansion coefficients contribute to the solution. Expansion coefficients for $\phi = \pi$ are shown in Fig. 4 for the same set of g values. We see very similar results except that the peaks all have the same phase.

4. Continuum Model

Our ability to calculate solutions to the eigenvalue is limited, even with the iterative algorithm discussed above, since we require even more expansion coefficients when g and Δn are large. From the results of the previous section, we see that the solutions do not change suddenly between different values of n, which suggests that we might be able to develop a continuum model. If so, then we would be able to extend the range over which we could obtain results even further.

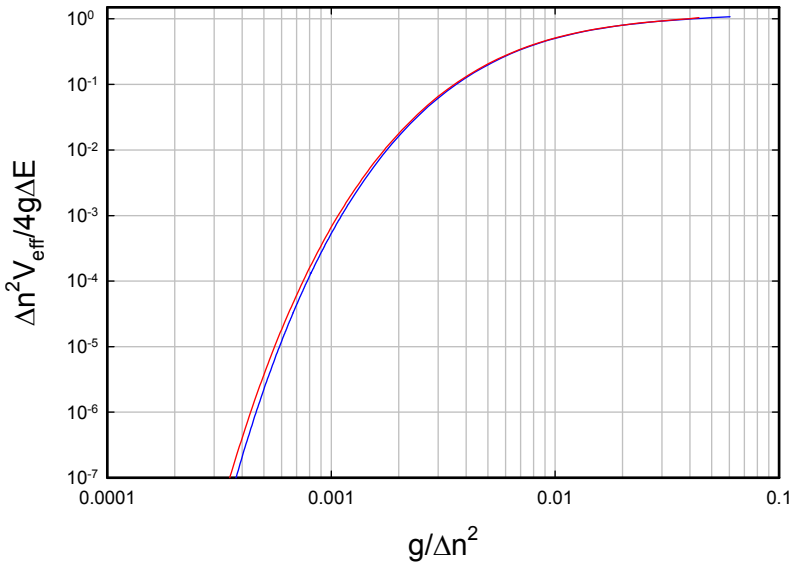

Figure 2. Scaled indirect coupling matrix element (derived from the level splitting) as a function of the $g/\Delta n^2$ for $\Delta n = 91$ (blue) and $\Delta n = 151$ (red).

4.1. Eigenvalue equation

To proceed, we define a continuous version of the index n according to

$$z = \frac{n}{\Delta n}. \tag{20}$$

The expansion coefficients v_n in the continuum approximation is then related to a continuous function $v(z)$ through

$$v_n = v\left(\frac{n}{\Delta n}\right). \tag{21}$$

The eigenvalue equation for $\phi = 0$ becomes

$$\begin{aligned}\epsilon_0 v(z) = {} & z v(z) + g\Bigg[v\left(z+1+\frac{1}{\Delta n}\right) + v\left(z+1-\frac{1}{\Delta n}\right) \\ & + v\left(z-1+\frac{1}{\Delta n}\right) + v\left(z-1-\frac{1}{\Delta n}\right)\Bigg].\end{aligned} \tag{22}$$

4.2. Approximate differential eigenvalue equation

Since the expansion coefficients vary slowly with n, we would expect reasonable results from assuming that $v(z)$ is locally continuous. For example, we can use a Taylor series expansion to write

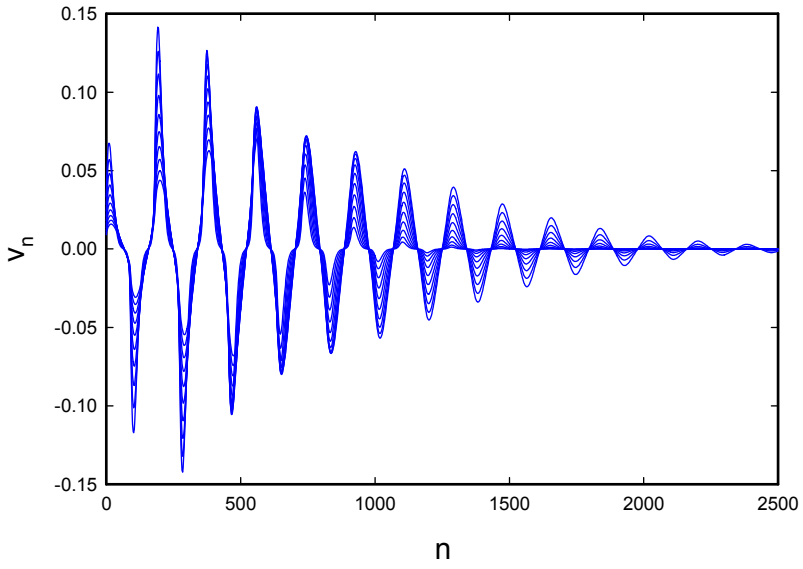

Figure 3. Results for the $\phi = 0$ expansion coefficients v_n for 10 values of g logarithmically spaced between $g = 10$ and $g = 100$. Results for $g = 10$ have the biggest magnitude for small n and the smallest magnitude for large n.

$$v\left(z + \frac{1}{\Delta n}\right) = v(z) + \frac{1}{\Delta n}\frac{\mathrm{d}v}{\mathrm{d}z} + \frac{1}{2\Delta n^2}\frac{\mathrm{d}^2 v}{\mathrm{d}z^2}, \tag{23}$$

$$v\left(z - \frac{1}{\Delta n}\right) = v(z) - \frac{1}{\Delta n}\frac{\mathrm{d}v}{\mathrm{d}z} + \frac{1}{2\Delta n^2}\frac{\mathrm{d}^2 v}{\mathrm{d}z^2}. \tag{24}$$

We can use these approximations to obtain an approximate difference-differential eigenvalue equation

$$\epsilon_0 v(z) = zv(z) + 2g[v(z+1) + v(z-1)] + \frac{g}{\Delta n^2}\frac{\mathrm{d}^2 v}{\mathrm{d}z^2}\bigg|_{z+1} + \frac{g}{\Delta n^2}\frac{\mathrm{d}^2 v}{\mathrm{d}z^2}\bigg|_{z-1}. \tag{25}$$

4.3. Discretization

To make progress, we would like to discretize the equation in order to obtain numerical solutions. Simple 3-point discretization results in

$$\begin{aligned}\epsilon_0 v_j &= z_j v_j + 2g[v_{j+N} + v_{j-N}] + \frac{g}{\Delta n^2}\frac{v_{j+N+1} - 2v_{j+N} + v_{j+N-1}}{\Delta z^2} \\ &\quad + \frac{g}{\Delta n^2}\frac{v_{j-N+1} - 2v_{j-N} + v_{j-N-1}}{\Delta z^2}.\end{aligned} \tag{26}$$

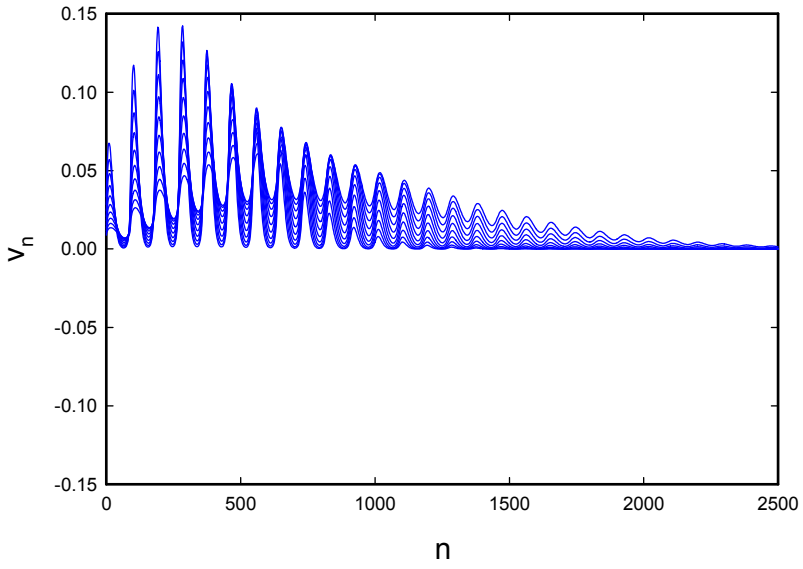

Figure 4. Results for the $\phi = \pi$ expansion coefficients v_n for 10 values of g logarithmically spaced between $g = 10$ and $g = 100$. Results for $g = 10$ have the biggest magnitude for small n and the smallest magnitude for large n.

The number of points used within a cycle N must satisfy

$$N \leq \Delta n \tag{27}$$

in order to obtain numerical solutions that correspond to the solutions of the original Hamiltonian.

4.4. Iterative solution

We have had some success using an iterative algorithm very similar to that discussed above to solve it. The correction equation that we used is

$$\epsilon \delta v_j = (z_j - 4\alpha_1 g)\delta v_j - \alpha_2 \frac{2g}{\Delta n^2}\left(\frac{\delta v_{j+1} - 2\delta v_j + \delta v_{j-1}}{\Delta z^2}\right) - r_j \tag{28}$$

with

$$\begin{aligned} r_j &= (z_j - \epsilon_0)v_j + 2g[v_{j+N} + v_{j-N}] + \frac{g}{\Delta n^2}\frac{v_{j+N+1} - 2v_{j+N} + v_{j+N-1}}{\Delta z^2} \\ &\quad + \frac{g}{\Delta n^2}\frac{v_{j-N+1} - 2v_{j-N} + v_{j-N-1}}{\Delta z^2}, \end{aligned} \tag{29}$$

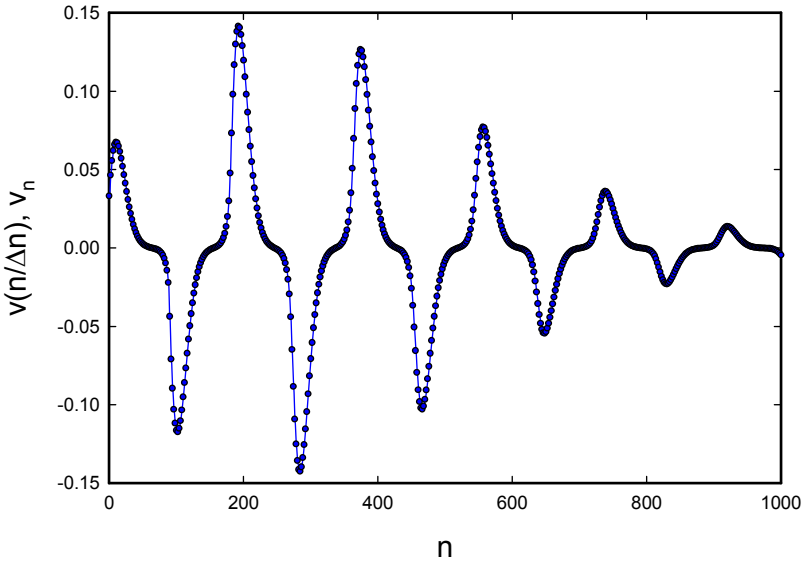

Figure 5. Results for the $\phi = 0$ expansion coefficients v_n computed for $g = 10$ using the periodic local model (black circles), and using the continuum approximation (blue line).

$$\alpha_1 = \frac{1}{2}, \quad \alpha_2 = 1 \tag{30}$$

and

$$v_j^{(m+1)} = v_j^{(m)} + \beta \delta v_j^{(m)} \tag{31}$$

with

$$\beta = 0.45. \tag{32}$$

The convergence rate is not great, but we are able to obtain solutions using this approach.

4.5. Numerical example

Of primary interest here is whether the solutions to the continuum model give a reasonable approximation to the solutions of the original problem. The issue here is that even though we now have more powerful tools to analyze the models, the number of coefficients involved in the solution grows in proportion to the product of g and Δn, so that we will end up needing to rely on a combination of analytic and numerical tools when Δn becomes large.

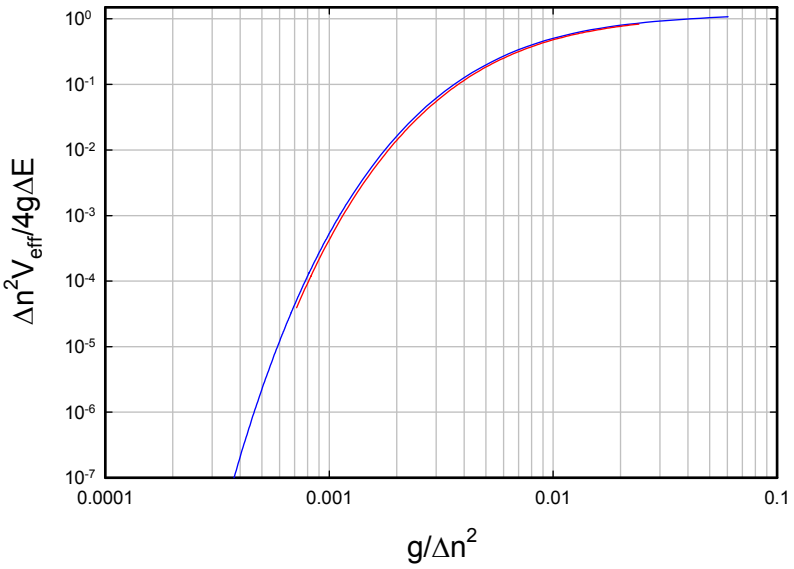

Figure 6. Scaled level splitting for $\Delta n = 91$ expressed as a scaled indirect matrix element from the periodic local model (blue line), and from the continuum approximation (red line).

In Fig. 5, we show the result from the continuum model (blue line) compared with the exact numerical coefficients from the periodic local model (black circles). The agreement is good, although there is a small offset associated with the continuum solution. The self-energy for the "exact" local periodic solution is

$$E(0) \;=\; -\,34.4370\;\Delta E. \tag{33}$$

The result from 3-pt differencing of the continuum approximation with 91 points is

$$E(0) \;=\; -\,34.4312\;\Delta E \;\; (3-\text{pt discretization}). \tag{34}$$

We can correct this self-energy by including the contribution of the lowest-order discretization error to obtain

$$E(0) \;=\; -\,34.4316\;\Delta E \;\; (\text{corrected } 3-\text{pt discretization}). \tag{35}$$

We conclude that the continuum model itself as an approximation is responsible for most of the energy difference.

The level splitting from the continuum model is shown in red in Fig. 6, compared with the periodic model result in blue. We see that the continuum model result is very close to the periodic model result. We conclude from these calculations that we should be able to make use of the continuum model for self-energy and for level splitting calculations and get good results.

5. Strong-coupling Limit

Direct numerical computations with the models described above becomes increasingly slow for larger values of g. This is because the solutions that make up the expansion coefficients include a large number of peaks, which involves a large number of points. An additional difficulty is that the iterative algorithm discussed converges more slowly as more points are used. It is possible to make use of the models outlined above to obtain systematic results for large g, by taking advantage of the presence of a large number of peaks. Since the peaks have nearly the same shape from one cycle to the next it becomes possible to develop strong coupling approximations.

5.1. Large g approximation for the periodic model

We see in Fig. 5 that the $\phi = 0$ solutions are made up of peaks that alternate in sign, and that for large g we might expect that the peak amplitudes will become uniform. In this case we would write

$$v_{n+\Delta n} \;=\; -\,v_n \;(\phi = 0). \tag{36}$$

The eigenvalue equation for the expansion coefficients in this limit reduces to

$$\epsilon_0 v_n \;=\; \frac{n}{\Delta n} v_n - 2g(v_{n+1} + v_{n-1}). \tag{37}$$

In the case of $\phi = \pi$, the different peaks have the same sign, so that we would expect

$$v_{n+\Delta n} \;=\; v_n \;(\phi = \pi). \tag{38}$$

The corresponding eigenvalue equation in this large g limit is essentially the same

$$\epsilon_\pi v_n \;=\; \frac{n}{\Delta n} v_n - 2g(v_{n+1} + v_{n-1}). \tag{39}$$

We show the result of computations for $\Delta n = 91$ for the level splitting as a function of g in Fig. 7 for this strong coupling approximation (red) compared with exact numerical results from the periodic model (blue). We see that the strong coupling approximation approaches the exact solution at large g, and that it deviates some at low g. This is consistent with our expectations, since when g is small only a few peaks make up the solution, in which case the assumption that the peaks are uniform (or linear) becomes poor.

5.2. Large g version of the continuum approximation

We can make a similar approximation in the case of the continuum approximation in the large g limit where there are many peaks, and where the shapes and amplitudes are similar in the different peaks. The resulting large g approximation is

$$\epsilon v(z) \;=\; z v(z) - 4g v(z) - \frac{2g}{\Delta n^2} \frac{\mathrm{d}^2 v}{\mathrm{d}z^2} \tag{40}$$

for both $\phi = 0$ and $\phi = \pi$.

This strong coupling continuum approximation is interesting because it predicts that the level splitting depends on the ratio $g/\Delta n^2$, but not on g independently. We can see this be recasting the eigenvalue equation as

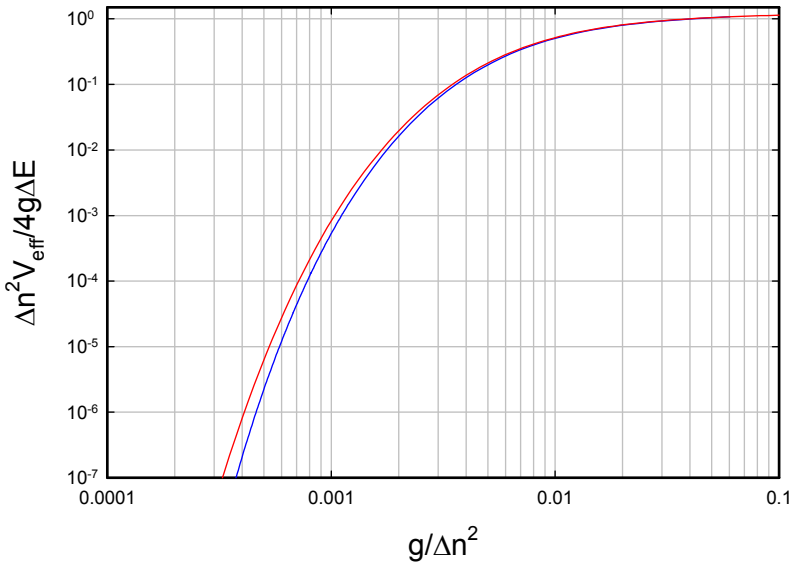

Figure 7. Scaled level splitting for $\Delta n = 91$ expressed as a scaled indirect matrix element from the periodic local model (blue line), and from the strong coupling approximation (red line).

$$\epsilon' v(z) \;=\; z v(z) - \frac{2g}{\Delta n^2}\frac{\mathrm{d}^2 v}{\mathrm{d}z^2}, \tag{41}$$

where

$$\epsilon' \;=\; \epsilon + 4g. \tag{42}$$

We noticed in our calculations that the discrete strong coupling approximation above gave very nearly the same level splittings as a function of $g/\Delta n^2$ for different large values of Δn. We see now that such behavior is expected, since when g is very large, it is only $g/\Delta n^2$ that matters in determining the level splitting.

The calculated level splitting in this model is very close to the large g approximation result in Fig. 7.

5.3. Scaling law for indirect coupling matrix element

From the strong coupling results, we see that the indirect coupling matrix element obeys a scaling law of the form

$$\frac{V_{\mathrm{eff}}}{\Delta E} \;=\; 4\frac{g}{\Delta n^2}\Phi\left(\frac{g}{\Delta n^2}\right). \tag{43}$$

For ease of use, we have fit the function $\Phi(x)$ according to

$$\Phi(x) \;=\; \exp\left\{a + b\ln x + c(\ln x)^2 + d(\ln x)^3 + e(\ln x)^4\right\} \tag{44}$$

using data in the range

$$0.00020 \;<\; x \;<\; 0.12. \tag{45}$$

The fitting parameters that result are

$$a \;=\; -1.11722, \quad b \;=\; -1.61939, \quad c \;=\; -0.780116, \quad d \;=\; -0.171302, \quad e \;=\; -0.0159906. \tag{46}$$

5.4. Analytic model for the large g continuum model

We can solve the differential equation for the strong coupling continuum model using a solution of the form

$$v(z) \;=\; \mathrm{Ai}\left[\left(\frac{\Delta n^2}{2g}\right)^{1/3}(z - z_0)\right], \tag{47}$$

$$\epsilon \;=\; -4g + z_0, \tag{48}$$

where Ai is an Airy function. A scaled version of this analytic result is shown in Fig. 8 compared with results from exact numerical calculations with the local periodic model. We see that the agreement over most of the cycle is very good. Deviations between the analytic solution and the exact solution on the small n side are due to the fact that the coefficients at $n - \Delta n$ are zero in the exact model (the analytic model here does not know about the cut-off at $n = 0$).

5.5. Peak amplitudes

If we assume that the different peaks have approximately the same shape, then it is possible to develop a model for the peak amplitudes. To proceed, we assume that the expansion coefficients for the $\phi = 0$ case can be approximated by

$$v_n \;=\; \sum_m (-1)^m a_m u_{n-m\Delta n}, \tag{49}$$

where a_m is the amplitude, and where u_n describes a single peak. For $\phi = 0$, the eigenvalue equation is

$$\epsilon_0 v_n \;=\; \frac{n}{\Delta n}v_n + g\Big[(v_{n+\Delta n+1} + v_{n+\Delta n-1}) + (v_{n-\Delta n+1} + v_{n-\Delta n-1})\Big], \tag{50}$$

we can develop an equation for the amplitudes of the form

$$\begin{aligned}\epsilon_0\langle u_n|u_n\rangle a_m \;=\; &\langle u_n|\frac{n}{\Delta n}|u_n\rangle - g\langle u_n|u_{n+1}\rangle a_{m+1} - g\langle u_n|u_{n-1}\rangle a_{m+1} \\ &-g\langle u_n|u_{n+1}\rangle a_{m-1} - g\langle u_n|u_{n-1}\rangle a_{m-1},\end{aligned} \tag{51}$$

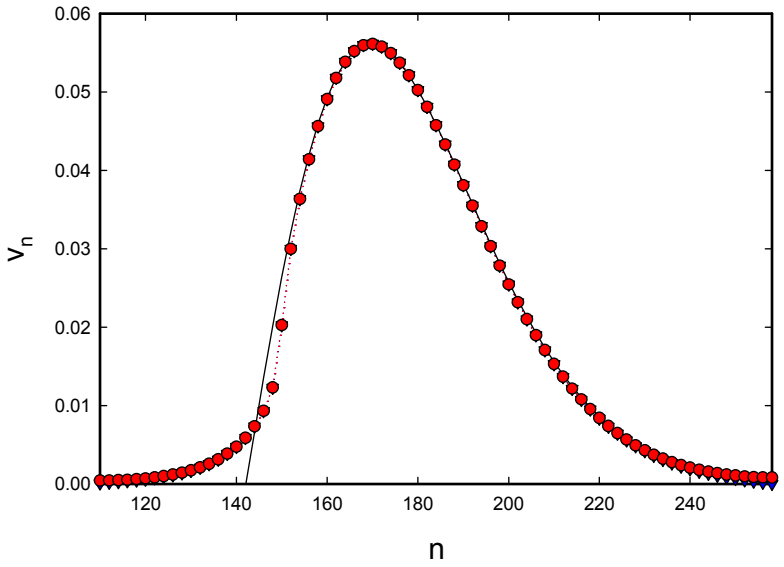

Figure 8. Expansion coefficients for $g = 30$ and $\Delta n = 151$; $\phi = 0$ (blue triangles); $\phi = \pi$ (red circles); and Airy function analytic model (black line).

When g is large we may approximate

$$\frac{\langle u_n | u_{n+1} \rangle}{\langle u_n | u_n \rangle} \rightarrow 1. \tag{52}$$

We require an estimate the expectation value $\langle n/\Delta n \rangle$. Since each successive peak occurs at a position Δn units past the previous one, we would expect that the expectation value would be equal to m plus an offset that depends on the width (which depends on $g/\Delta n^2$). From the results of numerical calculations, the following approximation seems reasonable

$$\left\langle \frac{n}{\Delta n} \right\rangle = m + \delta n \left(\frac{g}{\Delta n^2} \right). \tag{53}$$

We can then reduce the amplitude equation to

$$\left[\epsilon_0 - \delta n \left(\frac{g}{\Delta n^2} \right) \right] a_m = m a_m - 2g(a_{m-1} + a_{m+1}). \tag{54}$$

This equation can be solved analytically using a solution of the form

$$a_m = J_{m+m_0}(4g), \tag{55}$$

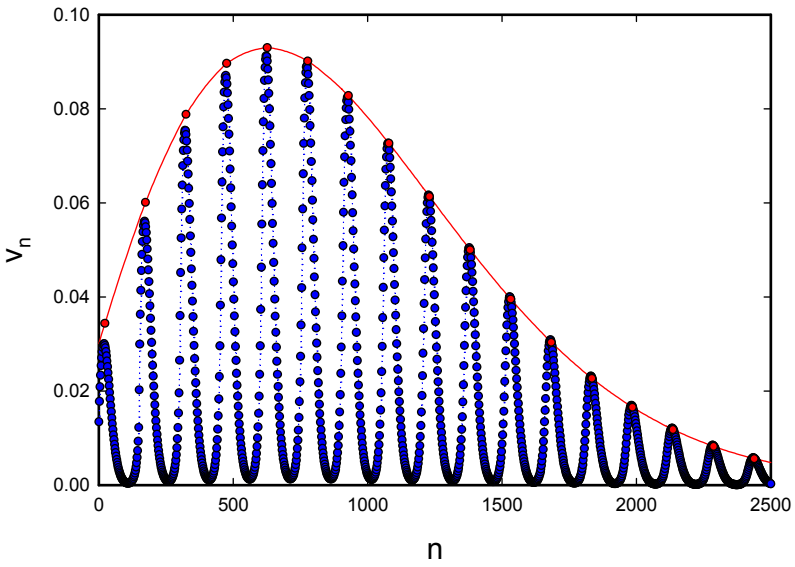

Figure 9. Expansion coefficients for $g = 30$, $\Delta n = 151$, and $\phi = \pi$ (blue); and results from the peak amplitude model (red).

where m_0 is chosen so that the first zero of the Bessel function is matched to the boundary condition near $n = 0$. We illustrate in Fig. 9 an example where we have chosen the $\phi = \pi$ version of the problem (in which the peaks all have the same sign, so that it is easier to compare). In this case, we have used $\Delta n = 151$ and $g = 30$, and we have scaled the amplitudes to approximately match the peak amplitude. We see that this model for the amplitudes is in reasonable agreement with the exact numerical calculation.

5.6. Continuum approximation for the peak amplitudes

When g becomes large there occur a great many peaks. In this case, we can adopt a continuum approximation

$$a_m \;\rightarrow\; a(m) \tag{56}$$

with

$$a_{m+1} \;\rightarrow\; a(m) + \frac{\mathrm{d}a}{\mathrm{d}m} + \frac{1}{2}\frac{\mathrm{d}^2 a}{\mathrm{d}m^2} \tag{57}$$

$$a_{m-1} \;\rightarrow\; a(m) - \frac{\mathrm{d}a}{\mathrm{d}m} + \frac{1}{2}\frac{\mathrm{d}^2 a}{\mathrm{d}m^2}. \tag{58}$$

The eigenvalue equation becomes

$$\left[\epsilon_0 + 4g - \delta n\left(\frac{g}{\Delta n^2}\right)\right] a(m) \;=\; ma(m) - 2g\frac{\mathrm{d}^2 a}{\mathrm{d}m^2}. \tag{59}$$

This is solved using

$$a(m) \;=\; \mathrm{Ai}\left[\left(\frac{1}{2g}\right)^{1/3}(m - \delta m)\right]. \tag{60}$$

Here δm is chosen to match the boundary condition.

6. Dynamics for Strong Coupling

Since the indirect coupling matrix element obeys a scaling law in the strong coupling limit, it is possible to examine coherent energy exchange under conditions where a large number of oscillator quanta are converted. From previous work the dynamics is governed by

$$\frac{\mathrm{d}^2}{\mathrm{d}t^2}m \;=\; \frac{2}{\hbar^2}\frac{\mathrm{d}}{\mathrm{d}m}V^2(m). \tag{61}$$

We assume in writing this that there are enough two-level systems present so that the nearly-degenerate set of indirectly coupled states can be treated as degenerate. To proceed, we recall that

$$g \;=\; \frac{V\sqrt{n}\sqrt{S^2 - m^2}}{\Delta E}. \tag{62}$$

In what follows we will simplify things by assuming that n does contribute to the dynamics. This would be the case if a large n were imposed such that the energy exchange gives rise to only a small change in oscillator excitation. This limit might also be of interest if conventional oscillator loss limited the maximum excitation of the oscillator.

6.1. Scaled Dicke number

In what follows, it will be convenient to work with a scaled version of m; hence, we define y according to

$$y \;=\; \frac{m}{S}. \tag{63}$$

The equation of motion can then be written as

$$\frac{\mathrm{d}^2}{\mathrm{d}t^2}y(t) \;=\; \frac{2}{\hbar^2 S^2}\frac{\mathrm{d}}{\mathrm{d}y}\left[4\Delta E\frac{g}{\Delta n^2}\Phi\left(\frac{g}{\Delta n^2}\right)\right]^2. \tag{64}$$

We can simplify the subsequent algebra if we introduce g_{max} which we define as

$$g_{\mathrm{max}} \;=\; \frac{V\sqrt{n}S}{\Delta E}. \tag{65}$$

This allows us to write

$$\frac{\mathrm{d}^2}{\mathrm{d}t^2}y(t) \;=\; \frac{32}{S^2}\left(\frac{\Delta E}{\hbar}\right)^2 \frac{\mathrm{d}}{\mathrm{d}y}\left[\left(\frac{g_{\max}}{\Delta n^2}\right)^2 (1-y^2)\Phi^2\left(\frac{g_{\max}}{\Delta n^2}\sqrt{1-y^2}\right)\right]. \tag{66}$$

6.2. Characteristic frequency

The scaling law here involves y appearing in the same way in the different terms. We can extract the physical parameters by introducing the scaled variable

$$\xi \;=\; \frac{g_{\max}}{\Delta n^2}\sqrt{1-y^2}. \tag{67}$$

This allows us to write

$$\frac{\mathrm{d}^2}{\mathrm{d}t^2}y(t) \;=\; \frac{32}{S^2}\left(\frac{\Delta E}{\hbar}\right)^2 \frac{\mathrm{d}}{\mathrm{d}y}\left[\xi^2\Phi^2(\xi)\right] \;=\; \frac{32}{S^2}\left(\frac{\Delta E}{\hbar}\right)^2 \frac{\mathrm{d}\xi}{\mathrm{d}y}\frac{\mathrm{d}}{\mathrm{d}\xi}\left[\xi^2\Phi^2(\xi)\right]. \tag{68}$$

We can evaluate the derivative in y to obtain

$$\frac{\mathrm{d}\xi}{\mathrm{d}y} \;=\; -\frac{g_{\max}}{\Delta n^2}\frac{y}{\sqrt{1-y^2}}. \tag{69}$$

This leads to

$$\frac{\mathrm{d}^2}{\mathrm{d}t^2}y(t) \;=\; -\frac{32}{S^2}\left(\frac{\Delta E}{\hbar}\right)^2 \left(\frac{g_{\max}}{\Delta n^2}\right)^2 y\left(\frac{1}{\xi}\frac{\mathrm{d}}{\mathrm{d}\xi}\left[\xi^2\Phi^2(\xi)\right]\right). \tag{70}$$

We can define a characteristic frequency Ω_0 for this model to satisfy

$$\Omega_0^2 \;=\; \frac{1}{S^2}\left(\frac{\Delta E}{\hbar}\right)^2 \left(\frac{g_{\max}}{\Delta n^2}\right)^2. \tag{71}$$

This can be recast as

$$\Omega_0^2 \;=\; \frac{1}{\Delta n^4}\left(\frac{V\sqrt{n}}{\hbar}\right)^2. \tag{72}$$

The characteristic frequency Ω_0 can then be written in the two equivalent forms

$$\Omega_0 \;=\; \frac{1}{S}\left(\frac{\Delta E}{\hbar}\right)\left(\frac{g_{\max}}{\Delta n^2}\right) \;=\; \frac{1}{\Delta n^2}\left(\frac{V\sqrt{n}}{\hbar}\right). \tag{73}$$

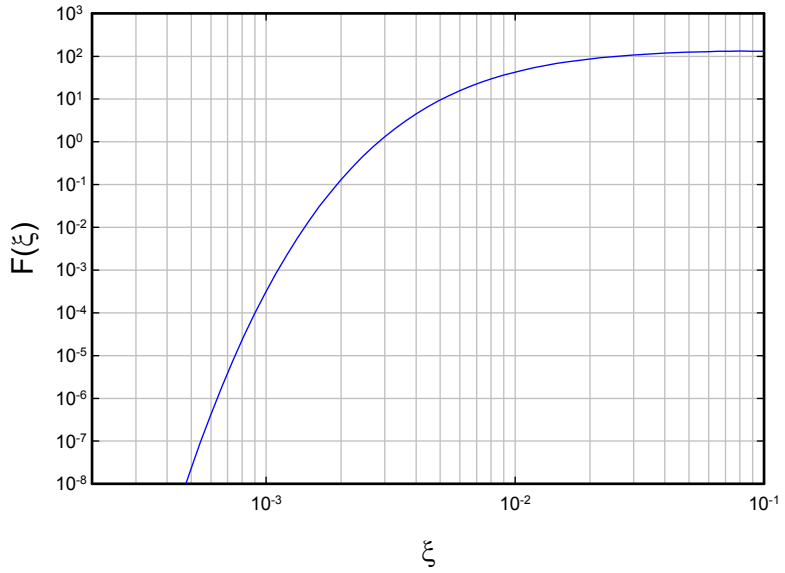

Figure 10. Function $F(\xi)$ discussed in the text plotted as a function of ξ.

6.3. Nonlinearity

Ultimately we end up with the dynamics of a nonlinear oscillator which can be expressed as

$$\frac{\mathrm{d}^2}{\mathrm{d}t^2}y(t) \;=\; -\,\Omega_0^2 y\left(\frac{32}{\xi}\frac{\mathrm{d}}{\mathrm{d}\xi}\left[\xi^2\Phi^2\left(\xi\right)\right]\right). \tag{74}$$

To compute the dynamics of this system, it is convenient to define

$$F(\xi) \;=\; \frac{32}{\xi}\frac{\mathrm{d}}{\mathrm{d}\xi}\left[\xi^2\Phi^2\left(\xi\right)\right]. \tag{75}$$

We have evaluated this function (see Fig. 10), and fit it to the form

$$F(\xi) \;=\; \exp\left\{a + b\ln\xi + c(\ln\xi)^2 + d(\ln\xi)^3 + e(\ln\xi)^4\right\} \tag{76}$$

with

$$a \;=\; 2.46013,\;\; b \;=\; -\,3.22909,\;\; c \;=\; -\,1.60184,\;\; d \;=\; -\,0.362187,\;\; e \;=\; -\,0.0332753. \tag{77}$$

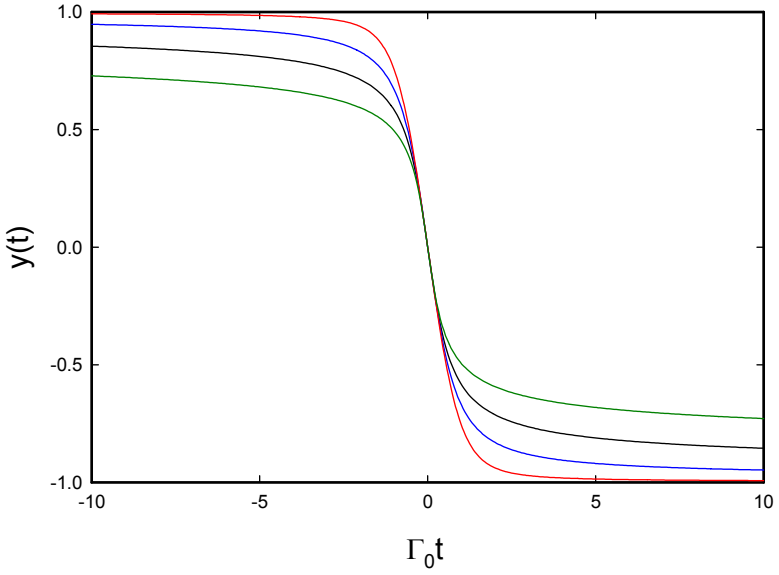

Figure 11. Non-periodic solutions for $y(t)$ as a function of scaled time for $g_{\max}/\Delta n^2$ values of 0.0003 (green), 0.001, 0.003, 0.01 (red). The time scaling uses $\tau^{-1} = |y'(0)|$.

6.4. Solutions

Using this function we may write for the evolution equation

$$\frac{\mathrm{d}^2}{\mathrm{d}t^2} y(t) \;=\; -\,\Omega_0^2 y F\left(\frac{g_{\max}}{\Delta n^2}\sqrt{1-y^2}\right). \tag{78}$$

In Fig. 11, we show non-periodic solutions that we computed for different values of $g_{\max}/\Delta n^2$. We scaled the time axis of the different solutions by the maximum rate for the different cases in order to compare them. To do this, we start with the maximum reaction velocity

$$\left|\frac{\mathrm{d}m}{\mathrm{d}t}\right|_{\max} \;=\; \frac{2}{\hbar}\max\{V_{\mathrm{eff}}\} \;=\; 8\left(\frac{\Delta E}{\hbar}\right)\left(\frac{g_{\max}}{\Delta n^2}\right)\Phi\left(\frac{g_{\max}}{\Delta n^2}\right). \tag{79}$$

The maximum rate for the normalized version of m can be written as

$$\Gamma_0 \;=\; \frac{1}{S}\left|\frac{\mathrm{d}m}{\mathrm{d}t}\right|_{\max} \;=\; \frac{8}{S}\left(\frac{\Delta E}{\hbar}\right)\left(\frac{g_{\max}}{\Delta n^2}\right)\Phi\left(\frac{g_{\max}}{\Delta n^2}\right) \;=\; \sqrt{2}\Omega_0\Phi\left(\frac{g_{\max}}{\Delta n^2}\right). \tag{80}$$

6.5. Connection between the maximum rate and the coupling

One of the key questions that relates to these models concerns determining how large the coupling matrix element must be in order for coherent energy exchange to occur at a given rate. In the large Δn scaling that we have considered in this section, we can determine the maximum reaction rate from the coupling matrix element by expressing Ω_0 in terms of V in the expression above to obtain

$$\Gamma_0 \;=\; \sqrt{2}\frac{1}{(\Delta n)^2}\frac{V\sqrt{n}}{\hbar}\Phi\left(\frac{g_{\max}}{(\Delta n)^2}\right). \tag{81}$$

The coupling matrix element in this model is $V\sqrt{n}$, so it is natural to expect $V\sqrt{n}/\hbar$ as providing the underlying rate scale. The maximum rate is then smaller by a factor of $(\Delta n)^2$, which is essentially the penalty in this model for fractionating the large two-level system quantum ΔE into a large number of oscillator quanta with energy $\hbar\omega_0$. The function Φ is shown in Fig. 7, and we might regard this factor as an additional penalty factor required for insufficiently strong coupling. Finally, we need to arrange for $g_{\max}/(\Delta n)^2$ to be sufficiently large so that our penalty Φ is not too great, which we can interpret as a constraint on the number of two-level systems required to fractionate the large quantum.

7. Discussion and Conclusions

The lossy spin-boson model is interesting in that it exhibits a strong coherent energy exchange effect between a set of two-level systems and an oscillator under conditions where the large energy quantum of the two-level systems is divided into a large number of oscillator quanta. In previous papers, we have examined this using perturbation theory [10], and using a second-order formulation [12]. Our interest in the problem stems from seeking models for the excess heat effect in the Fleischmann–Pons experiment, where we interpret the experimental results as splitting a large nuclear quantum of energy into a very large number of atomic scale quanta associated with phonon modes of the lattice. We are interested in this paper in the question of whether the lossy spin-boson model is capable coherent energy exchange under such conditions.

In a previous paper we introduced the periodic local approximation [13], which is a powerful tool which allows us to reduce a large and difficult two-dimensional (m and n) problem into a much smaller and easier one-dimensional (n) problem when a resonance condition is satisfied. In this paper we have exploited the local approximation to compute eigenfunctions, self-energies, and indirect coupling matrix elements for examples when the dimensionless coupling constant is reasonably large and when many oscillator quanta are exchanged. After a number of such calculations, we have found that the system appears to obey a scaling law for the self-energy, and a scaling law for the indirect coupling matrix element. The is interesting in its own right, since we had no reason *a priori* to expect such behavior. Also interesting is that the self-energy and indirect matrix elements show convergence to the strong coupling limit result in a regime where we can perform calculations directly, enabling us to verify the behavior of the system independently.

With the aid of the scaling law for the indirect coupling matrix element, we are able to carry out computations of the resulting system dynamics in the strong coupling regime where coherent energy exchange occurs with a very large number of oscillator quanta. In the end, we see that this lossy spin-boson model is able to exchange energy efficiently even when the two-level system transition energy is very much less than the characteristic energy of the oscillator. For this to work, the system must be in a very strong coupling regime, which can be done by simply increasing the number of two-level systems. The price to be paid for such a large mismatch is a reduction in the coherent energy transfer rate. In the large n model, the rate Γ_0 scales as $(\Delta n)^{-2}$ when Δn is increased and $g_{\max}/\Delta n^2$ is held fixed. Such scaling is relatively gentle, which encourages us in exploring it for application to excess heat in the Fleischmann–Pons experiment. The coherent energy transfer rate in the finite n model discussed in the Appendix is much faster.

In looking forward, much work remains to develop a usable theory for the Fleischmann–Pons experiment. We will need to generalize the model to describe donor and receiver two-level (as well as n-level) systems. Our computations in this paper were carried out in an infinite loss approximation, and we will need to develop models with finite oscillator loss at ΔE in order to connect with experiment. In our computations in the strong coupling limit in this work, a characteristic feature of the solutions is that a very large number of different oscillator n-states are occupied when g is large. In the physical system the oscillator sees loss at ω_0, so that one would expect the results to depend on this loss. We would like to examine models which shed light on this. We will also need to connect this simple two-level system and oscillator models to the physical system, which will require a derivation of the model as well as an evaluation of the coupling matrix elements.

Appendix A. A Finite n Model

We chose the simple model discussed in the previous subsections in part because it was simple and informative. However, the restriction that the number of oscillator quanta is not changed by the dynamics is a strong one, and we are interested here in the generalization to the case where the change in the number of oscillator quanta is significant.

Appendix A.1. Energy conservation

In this case, the number of oscillator quanta n would depend explicitly on m. If we assume that the oscillator loss at ω_0 can be neglected, then we may use energy conservation to write

$$n_0 \;=\; n + \Delta n(S+m). \tag{A.1}$$

In this model the number of oscillator quanta decreases when the number of excited two-level systems increases.

Appendix A.2. Evolution equation

The relation between the local g and m is modified to read

$$g \;=\; \frac{V\sqrt{n_0-\Delta n(S+m)}\sqrt{S^2-m^2}}{\Delta E}. \tag{A.2}$$

We use this to generalized the definition of ξ to

$$\xi \;=\; \frac{g}{\Delta n^2} \;=\; \frac{VS\sqrt{n_0-\Delta nS(1+y)}\sqrt{1-y^2}}{\Delta E\Delta n^2}. \tag{A.3}$$

We then compute

$$\frac{\mathrm{d}\xi}{\mathrm{d}y} \;=\; -\frac{g}{\Delta n^2}\left[\frac{y}{1-y^2}+\frac{S\Delta n}{2n}\right], \tag{A.4}$$

where we note that g and n both depend on y.

The evolution equation in general can be written as

$$\frac{\mathrm{d}^2}{\mathrm{d}t^2}y(t) \;=\; \frac{32}{S^2}\left(\frac{\Delta E}{\hbar}\right)^2\frac{\mathrm{d}\xi}{\mathrm{d}y}\frac{\mathrm{d}}{\mathrm{d}\xi}\left[\xi^2\Phi^2\left(\xi\right)\right]. \tag{A.5}$$

Using the expression above for the derivative $d\xi/dy$, we obtain

$$\frac{d^2}{dt^2}y(t) \;=\; -\frac{V^2 n}{\hbar^2 \Delta n^4}\left[y + \frac{S\Delta n}{2n}(1-y^2)\right]F(\xi). \tag{A.6}$$

Note that n and ξ depend explicitly on y in this evolution equation.

Appendix A.3. Steady-state condition

If all of the two-level systems are initialized in the ground state, and if the oscillator is initialized in an excited state, we would expect that some of the two-level systems would become excited. We can determine how many are excited in the steady state by solving

$$y + \frac{S\Delta n}{2n}(1-y^2) \;=\; 0. \tag{A.7}$$

We use

$$n \;=\; n_0 - \Delta n S(1+y) \tag{A.8}$$

to obtain the constraint

$$3y^2 + 2\left(1 - \frac{n_0}{\Delta n S}\right) - 1 \;=\; 0. \tag{A.9}$$

We assume that the amount of excitation is small, and obtain the approximate result

$$y \;=\; -1 + \frac{n_0}{2\Delta n S}. \tag{A.10}$$

The number of excited two-level systems in this case is

$$m + S \;=\; \frac{1}{2}\frac{n_0}{\Delta n} \;=\; \frac{n}{\Delta n}. \tag{A.11}$$

This is the condition at which the contributions that increase the indirect matrix elements are the same for the two-level systems as for the oscillator.

Appendix A.4. Discussion

In the large n model described in Section 6, if the oscillator is initially excited and the two-level systems are in the ground state, then the model predicts that in time all of the two-level systems would be excited. One of the reasons for going to a finite n model is that now the matrix elements increase when the number of oscillator quanta increases, so that the two-level systems in such a model want to give up their energy to the oscillator. In this new model, the rate at which the two-level systems give up their energy is increased by roughly $S\Delta n/n$ over that of the large n limit, a factor which can be very large.

If the two-level systems are initially in the ground state, then we would expect that they can be excited if the oscillator is highly excited. The evolution equation for this model gives this result. The large n model and this energy

conserving finite n model exhibit two different limits for coherent energy exchange. Unfortunately, there are issues with both models in connection with modeling excess heat in the Fleischmann—Pons experiment. If we are interested in coupling energy to optical phonon modes, it can never be the case that the system can reach a large n limit, because the associated thermal power would be so high as to be physically unreasonable (since the thermalization time of these phonon modes is so short). Since optical phonon modes are so lossy, a model which enforces energy conservation without optical phonon loss also seems not so realistic. To do better, we will need to include phonon loss.

References

[1] M. Fleischmann, S. Pons and M. Hawkins, *J. Electroanal Chem.* **201** (1989) 301; errata, **263** (1990) 187.
[2] M. Fleischmann, S. Pons, M.W. Anderson, L.J. Li and M. Hawkins, *J. Electroanal. Chem.* **287** (1990) 293.
[3] M.H. Miles, R.A. Hollins, B.F. Bush, J.J. Lagowski and R.E. Miles, *J. Electroanal. Chem.* **346** (1993) 99.
[4] M.H. Miles, B.F. Bush and J.J. Lagowski, *Fusion Technol.* **25** (1994) 478.
[5] M.H. Miles, Correlation of excess enthalpy and helium-4 production: A review, *Proc. ICCF10*, 2004, p. 123.
[6] P.L. Hagelstein, M.C.H. McKubre, D.J. Nagel, T.A. Chubb and R.J. Hekman, New physical effects in metal deuterides, *Proc. ICCF11*, 2005, p. 23.
[7] P.L. Hagelstein, *Naturwissenschaften* **97** (2010) 345.
[8] D. Letts, D. Cravens and P.L. Hagelstein, Dual laser stimulation and optical phonons in palladium deuteride, in low-energy nuclear reactions and new energy technologies, *Low-Energy Nuclear Reactions Sourcebook*, Vol. 2, American Chemical Society, Washington, DC, 2009, p. 81.
[9] P.L. Hagelstein, D. Letts and D. Cravens, Terahertz difference frequency response of PdD in two-laser experiments, *J. Cond. Mat. Nucl. Sci.* **3** (2010) 59.
[10] P.L. Hagelstein and I.U. Chaudhary, Energy exchange in the lossy spin-boson model, *J. Cond. Mat. Nucl. Sci.* **5** (2011) 52.
[11] P.L. Hagelstein and I.U. Chaudhary, Dynamics in the case of coupled degenerate states, *J. Cond. Mat. Nucl. Sci.* **5** (2011) 72.
[12] P.L. Hagelstein and I.U. Chaudhary, Second-order formulation and scaling in the lossy spin-boson model, *J. Cond. Mat. Nucl. Sci.* **5** (2011) 87.
[13] P.L. Hagelstein and I.U. Chaudhary, Local approximation for the lossy spin-boson model, *J. Cond. Mat. Nucl. Sci.* **5** (2011) 102.